Chapter II. Tunable interplay between epidermal growth factor and cell-cell contact governs the spatial dynamics of epithelial growth

Abstract

Contact-inhibition of proliferation constrains epithelial tissue growth, and the loss of contact-inhibition is a hallmark of cancer cells. In most physiological scenarios, cell-cell contact inhibits proliferation in the presence of other growth-promoting cues, such as soluble growth factors (GFs). How cells quantitatively reconcile the opposing effects of cell-cell contact and GFs, such as epidermal growth factor (EGF), remains unclear. Here, using quantitative analysis of single cells within multicellular clusters, we show that contact is not a "master switch" that overrides EGF. Only when EGF recedes below a threshold level, contact inhibits proliferation, causing spatial patterns in cell cycle activity within epithelial cell clusters. Furthermore, we demonstrate that the onset of contact-inhibition and the timing of spatial patterns in proliferation may be re-engineered. Using micropatterned surfaces to amplify cell-cell interactions, we induce contact-inhibition at a higher threshold level of EGF. Using a complementary molecular genetics approach to enhance cell-cell interactions by overexpressing E-cadherin also increases the threshold level of EGF at which contact-inhibition is triggered. These results lead us to propose a phase diagram in which epithelial cells transition from a contact-uninhibited state to a contact-inhibited state at a critical threshold level of GF, a property that may be tuned by modulating the extent of cell-cell contacts. This new quantitative model of contact-inhibition has direct implications for how tissue size may be determined and deregulated

during development and tumor formation, respectively, and provides design principles for engineering epithelial tissue growth in applications such as tissue engineering.

Reprinted from Kim, J.-H., K. Kushiro., N.A. Graham, and A.R. Asthagiri from *Proceedings of the National Academy of Sciences USA* (2009)

Introduction

Contact-inhibition of proliferation is a key constraint on the growth of epithelial tissues. The loss of contact-inhibition is a hallmark of cancer cells, leading to hyperproliferation of epithelial cells and tumor formation (1). In physiological scenarios, cell-cell contact inhibits proliferation in the presence of other growth-promoting environmental cues, such as soluble growth factors (GFs). However, how cells quantitatively reconcile these conflicting cues to make a "net decision" on cell cycle commitment remains unclear. Does cell-cell contact act as a potent switch that supercedes the stimulatory effect of GFs? Or, is there a quantitative titration between the extent of cell-cell contact and the amount of GFs that ultimately determines cell cycle activity?

Whether cells evaluate contact and GFs in a binary or graded manner has important implications for our understanding of cancer progression. Cancers develop through multiple molecular "hits." Each hit may modify how cells weigh the opposing effects of contact and GFs. Thus, the loss of contact-inhibition may occur progressively with gradations of deregulation building up over the course of oncogenesis. Whether the loss of contact-inhibition should be viewed from this quantitative perspective or from the more classical binary viewpoint remains unclear because the quantitative interplay between contact and GFs in regulating cell cycle activity remains to be elucidated.

A principal challenge to gauging the quantitative crosstalk between contact and GFs is that the underlying mechanisms are arranged into a complex physiochemical network. The cadherin family of transmembrane cell surface proteins plays a critical role (2). Both ectopic expression of cadherins and exposure to beads coated with cadherins arrest cell cycle activity (3-8). Cadherins in association with other membrane proteins, such as Merlin, bind and regulate the trafficking of growth factor receptors (9-12). In addition, cadherins regulate contact-inhibition through mechanotransduction pathways. Cadherin-mediated contacts are coupled to the actin cytoskeleton (2, 13) and alter the distribution of traction forces between the cell and the substratum. Thus, in the interior of multicellular clusters where cell-cell contacts are abundant, the traction forces are minimal, and cell cycle activity is inhibited (14). Assessing the integrated performance of these chemical and physical mechanisms is non-trivial and leaves open a systems-level question: How do cells quantitatively evaluate cell-cell contact and GFs to regulate cell cycle commitment?

To address this question, we undertook a quantitative experimental analysis of cell cycle activity of individual epithelial cells within multicellular clusters. We show that a quantitative titration of the amount of epidermal growth factor (EGF) and the level of cell-cell contact regulates cell cycle activity. Only below a critical threshold level of EGF, cadherin-mediated contacts suppress cell proliferation. Moreover, we demonstrate that this threshold amount of EGF is a tunable property. By manipulating cell-cell interactions using either micropatterned surfaces or molecular genetics, we induce contact-inhibition at a higher level of EGF. These findings suggest a new quantitative

model of contact-inhibition of proliferation: We propose a phase diagram in which epithelial cells transition from a contact-uninhibited state to a contact-inhibited state at a critical threshold level of GF, a property that may be tuned by modulating the extent of cell-cell contacts. This quantitative model of contact-inhibition has direct implications for how tissue size may be determined and deregulated during development and tumor formation, respectively, and provides design principles for engineering epithelial tissue growth in applications such as tissue engineering.

Results and Discussion

To examine the quantitative interplay between GFs and cell-cell contact in regulating cell proliferation, we quantified cell cycle activity in clusters of non-transformed mammary epithelial cells (MCF-10A) stimulated with different doses of EGF (Fig. 1A). In early time, BrdU uptake (a measure of DNA synthesis) was observed among cells both in the periphery and the center of clusters. Thus, cell-cell contact is not sufficient to halt cell cycle activity among interior cells at 24 h. Only later in time, BrdU uptake was localized to the periphery of cell clusters, while the growth of interior cells was impeded. This spatial pattern was especially evident at 48 and 72 h post-stimulation in cultures initially treated with 0.1 and 1 ng/ml EGF, respectively (Fig. 1A, panels d, h). Treatment with an E-cadherin function-blocking antibody eliminated the spatial pattern in cell cycle activity, while a non-specific mouse IgG had no effect (Fig. 1B). These results confirm that E-cadherin-mediated contact-inhibition triggers the spatial pattern in

proliferation and rules out alternative mechanisms, such as a diffusion-limited spatial gradient in EGF.

These results demonstrate that E-cadherin-mediated contact-inhibition induces spatial patterns in proliferation only at specific times in culture. Furthermore, cells stimulated with a higher dose of EGF take a longer time to exhibit spatial patterns in cell cycle activity (Fig. 1A, panels d and h). We reasoned that this apparent dependence of contact-inhibition on EGF dosage may be linked to receptor-mediated degradation of EGF. Upon binding its receptor, the EGF/EGF receptor complex is internalized and a fraction of the ligand is degraded in the lysosome (15). We hypothesized that the EGF concentration may have to dip to a critical threshold level in order for cell-cell contact to effectively suppress cell cycle activity of interior cells. Consistent with this hypothesis, in cultures treated with a high dose of EGF (10 ng/ml EGF), both interior and peripheral cells maintain equal levels of cell cycle activity at all three time points (24, 48, and 72 h) (Fig. S1). Furthermore, direct measurement of EGF concentration in the medium showed that the amount of EGF decreases by two to three orders-of-magnitude over time (Fig. 1C), revealing a significant rate of cell-mediated ligand depletion.

If contact-inhibition is in fact sensitized to a threshold EGF concentration, then this threshold ought to be independent of the initial dose of EGF. A closer examination of the EGF depletion data confirms this hypothesis. Regardless of the initial amount of EGF, approximately 3×10^3 EGF molecules/cell are present when spatial patterns in proliferation are observed (Fig. 1C). We note that the BrdU assay identifies cells that

have already committed to the cell cycle and are actively undertaking DNA synthesis. Based on the general timing of the cell cycle, the evaluation of environmental cues and the decision to enter the cell cycle likely occurred ~20 h earlier (16). Thus, we conclude that at the time when contacts inhibit cell cycle entry among interior cells, the critical threshold of EGF is approximately 3 x 10^4 molecules/cell.

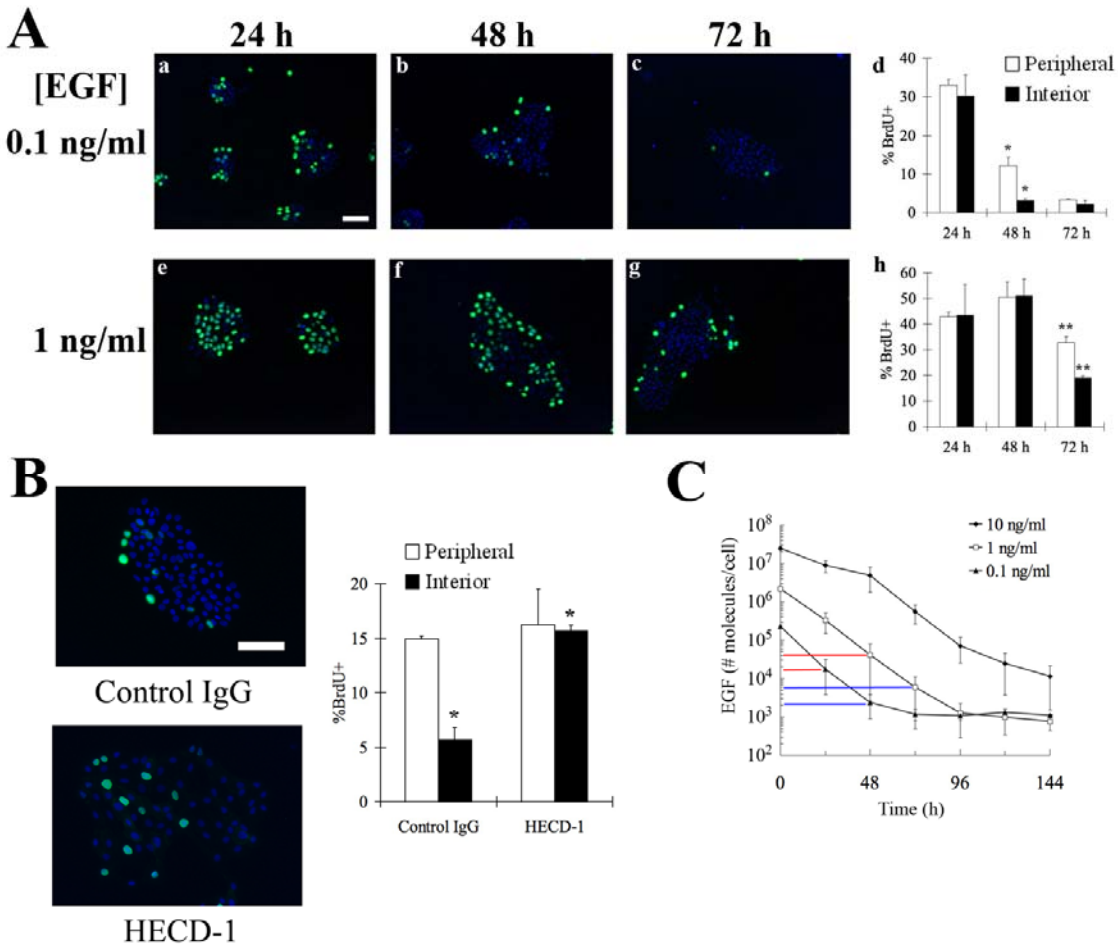

Figure 1. E-cadherin-mediated contact-inhibition triggers spatial patterns in cell cycle activity only when EGF depletes to a threshold concentration. (A) BrdU incorporation (green) and DAPI staining (blue) in MCF-10A cells initially seeded at 5x10^3 cell/cm^2 and treated with indicated doses of EGF for 24, 48 and 72 h. Panels d and

h show quantitation of the percentage of peripheral and interior cells incorporating BrdU. Error bars represent s.e.m. (n = 2-5). The *asterisk* and *double-asterisk* denote $p < 0.01$ and $p < 0.05$, respectively. (B) The effect of control IgG and anti-E-cadherin function blocking antibody on spatial pattern in cell cycle activity. Cells were treated with antibodies 24 h after stimulation with 0.1 ng/ml EGF. Twenty-four hours later, BrdU uptake (green) and DAPI (blue) was assessed. Percentage of peripheral and interior cells incorporating BrdU was quantified. Error bars indicate s.e.m. (n = 2). The *asterisk* indicates $p < 0.05$. (C) Amount of EGF in the medium for cultures treated initially with indicated doses of EGF. The vertical lines indicate the amount of EGF when a spatial pattern in proliferation is observed (blue) and 24 h prior (red). The error bars indicate s.e.m. (n = 2). The scale bar represents 100 μm.

To test further whether contact-inhibition occurs only at this critical EGF concentration, we designed an alternate approach to measure the threshold. Instead of waiting for ligand to deplete, we exposed cells to a broader range of EGF concentrations, including low levels that would emulate the late-depletion scenarios. Furthermore, we quantified cell cycle activity at a common time point, eliminating any changes in cells that could accumulate over time. In this assay at relatively high EGF concentrations (0.1, 1, and 10 ng/ml), both peripheral and central cells proliferate with nearly equal propensity (Fig. 2A and Fig. S3A). However, at lower EGF concentrations (0.001 and 0.01 ng/ml) BrdU uptake ceases selectively among interior cells, while peripheral cells maintain higher cell cycle activity. Thus, as in the previous assay format, contact-inhibition is triggered only when EGF dips below a critical threshold concentration (0.01

ng/ml). This threshold translates to ~10^4 EGF molecules/cell, demonstrating a common quantitative "setting" for contact-inhibition that is remarkably similar between the two assay formats.

We hypothesized that at this critical threshold level of EGF, cell-cell contact may be obstructing specific signaling pathways that are needed to stimulate cell cycle activity in interior cells. To examine this hypothesis, we focused on two major intracellular signals, Erk and Akt, that regulate cell cycle progression in many other cell systems (17) and are necessary for EGF-mediated proliferation in MCF-10A cells (Fig. S2). We quantified the activation of these signals in single cells at the periphery and interior of clusters. At relatively high EGF concentrations, Erk activation is uniform across the cluster (Fig. 2B and Fig. S3B). However, at 0.001 and 0.01 ng/ml EGF, the level of ppErk is distinctly higher in the peripheral cells (Fig. 2B and Fig. S3B). In contrast, Akt phosphorylation does not exhibit spatial heterogeneity at any of the EGF concentrations (Fig. 2C and Fig. S3C). Similar to Akt signaling, EGFR phosphorylation on Y1068 and Y1173 residues seemed to be uniform across the cell cluster for all EGF concentrations (Fig. S4). Thus, a spatial pattern in Erk signaling, but not Akt or EGFR phosphorylation, occurs at precisely the same threshold EGF dose at which contact inhibits cell cycle activity.

The emerging model from our data is that when the amount of EGF dips below a threshold value, cell-cell contact effectively inhibits EGF-mediated Erk signaling and thereby arrests cell cycle progression. If this model is accurate, supplying fresh ligand to

raise its concentration above the threshold should reverse spatial disparities in Erk signaling and cell cycle activity. To test this possibility, we treated serum-starved MCF-10A cells with 0.1 ng/ml EGF, and 24 h later, replenished the medium with fresh 0.1 ng/ml EGF. Following refreshment, the level of phosphorylated Erk in interior and peripheral cells was equivalent (Fig. S4A) in sharp contrast to the spatial pattern observed in non-replenished cultures (Fig. 2B). Furthermore, replenishing EGF entirely eliminates the spatial pattern in cell cycle activity (Fig. S4B). These results support our model and demonstrate that as EGF concentration dips below a threshold level, cadherin-mediated contacts selectively inhibit EGF-mediated Erk signaling and cell cycle activity among interior cells.

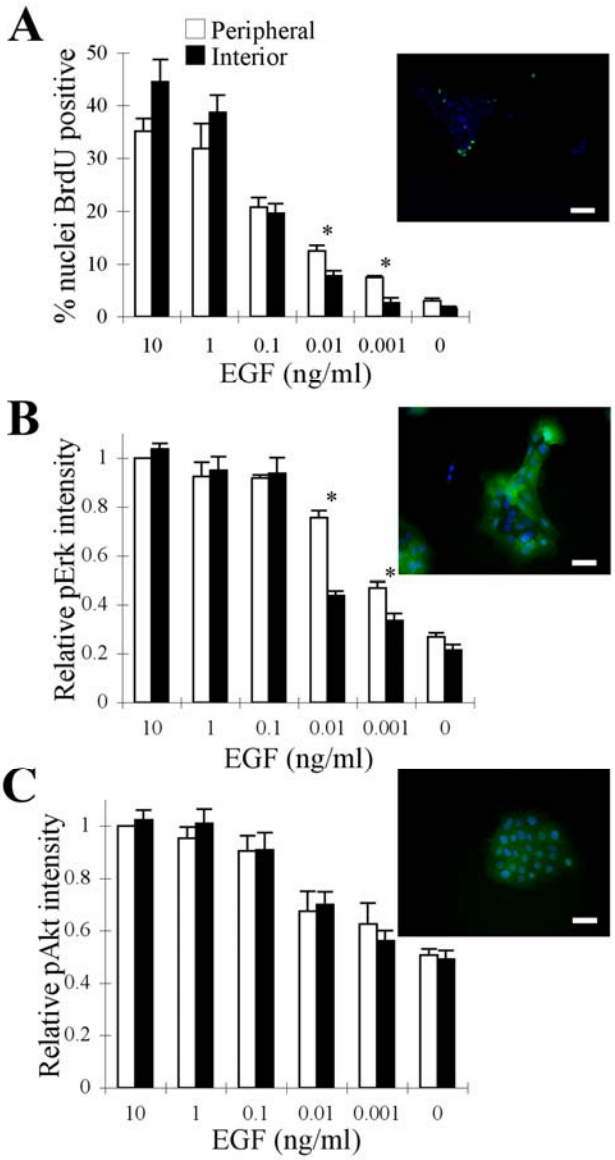

Figure 2: Selective attenuation of Erk, but not Akt, among interior cells correlates with contact-inhibition. MCF-10A cells seeded at a density of 10^4 cells/cm^2 were serum starved for 24 h and stimulated with the indicated doses of EGF or left untreated. BrdU uptake (A, green) and Erk/Akt (B/C, green) signals were assessed by immunostaining 24 h and 15 min, respectively, following EGF treatment. Nuclei were co-stained with DAPI (blue). Insets show representative images for cells treated with 0.01 ng/ml EGF. The bar graphs show percentage of nuclei incorporating BrdU (A), the relative nuclear intensity

of ppErk (B) and the relative nuclear intensity of pAkt (C) in peripheral and interior cells. Nuclear ppErk and pAkt intensities are reported relative to the amount of signal in peripheral cells treated with 10 ng/ml EGF. The *error bars* indicate s.e.m. (A: n=3, B: n=3, C: n=2). The *asterisks* denote $p < 0.05$. The scale bars represent (A) 100 μm and (B, C) 50 μm.

Furthermore, this threshold model seems relevant in other cell types. In Eph4 mouse mammary epithelial cells, when EGF level is increased above a threshold level, all cells in the cluster undergo DNA synthesis; meanwhile, a contact-inhibited pattern of proliferation is observed at the threshold amount of EGF (Fig. S6). Interestingly, the threshold in Eph4 cells occurs at approximately 1.5×10^3 EGF molecules/cell and is different from the threshold quantified in MCF-10A cells. Thus, while the interplay between EGF and contact seems to be a general feature, the quantitative set points for this threshold may vary across epithelial cell types.

In this manner, our analysis reveals a threshold amount of EGF at which contact-inhibition effectively induces a spatial pattern in cell cycle activity. An intriguing question is whether this competition operates bidirectionally. That is, instead of lowering EGF concentration to enable contact-inhibition, can cell-cell interactions be enhanced so that it competes more effectively with higher doses of EGF? Or, is the threshold EGF concentration a “hard-wired” parameter of contact-inhibition?

To examine this question, we first modulated cell-cell interactions using micropatterned substrates. By varying the number of cells seeded onto circular adhesive micropatterns of the same size, we manipulated the surface area of contact between neighboring cells (Fig. 3A). The density of DAPI staining confirmed the relative differences in cell density. Following stimulation with medium containing 20 ng/ml EGF, a spatial pattern in cell proliferation was evident in the culture with more extensive cell-cell interactions. Meanwhile, DNA synthesis in the low-density population was homogeneous. This result reveals that contact-inhibition of proliferation may be achieved at significantly higher doses of EGF if cell-cell interactions are augmented.

An important caveat, however, is that the growth arrest of interior cells in the high-density culture may be due to non-specific mechanical stresses at high cell density, space limitations due to overcrowding and/or reduced access to the underlying adhesive substrate. To determine whether cell-cell contacts are responsible for the observed spatial pattern in the high-density population, we examined the effect of downregulating E-cadherin expression using siRNA. Transfection with siRNA, but not a control construct, significantly reduced E-cadherin expression in MCF-10A cells (Fig. S6). Cells treated with the control siRNA and seeded at high density exhibited a spatial pattern in proliferation (Fig. 3B), revealing that the control siRNA treatment had no effect on contact-inhibition. In contrast, the spatial pattern was eliminated in cells plated at the same high density and treated with E-cadherin siRNA. These results demonstrate that E-cadherin plays a critical role in mediating the observed contact-inhibition on micropatterned substrates at higher doses of EGF. It remains unclear, however, whether

E-cdherin itself directly delivers the contact inhibition signal or whether E-cadherin interactions are needed to establish sufficient cell-cell contact for other proteins to mediate the contact inhibition signal. Indeed, the region of cell-cell contact is a rich environment of intercellular signaling involving proteins, such as Notch and ephrins, that may play a critical role in cell cycle regulation.

Our results suggest a quantitative phase diagram in which epithelial cells reside in two possible states: contact-uninhibited and contact-inhibited states (Fig. 3C). The transition into the contact-inhibited state occurs when the amount of EGF recedes below a critical threshold level. Furthermore, we showed that amplifying the level of cell-cell interactions using a micropatterned surface enables contact-inhibition at a higher level of EGF, suggesting that the tipping point at which contact-inhibition is triggered is tunable.

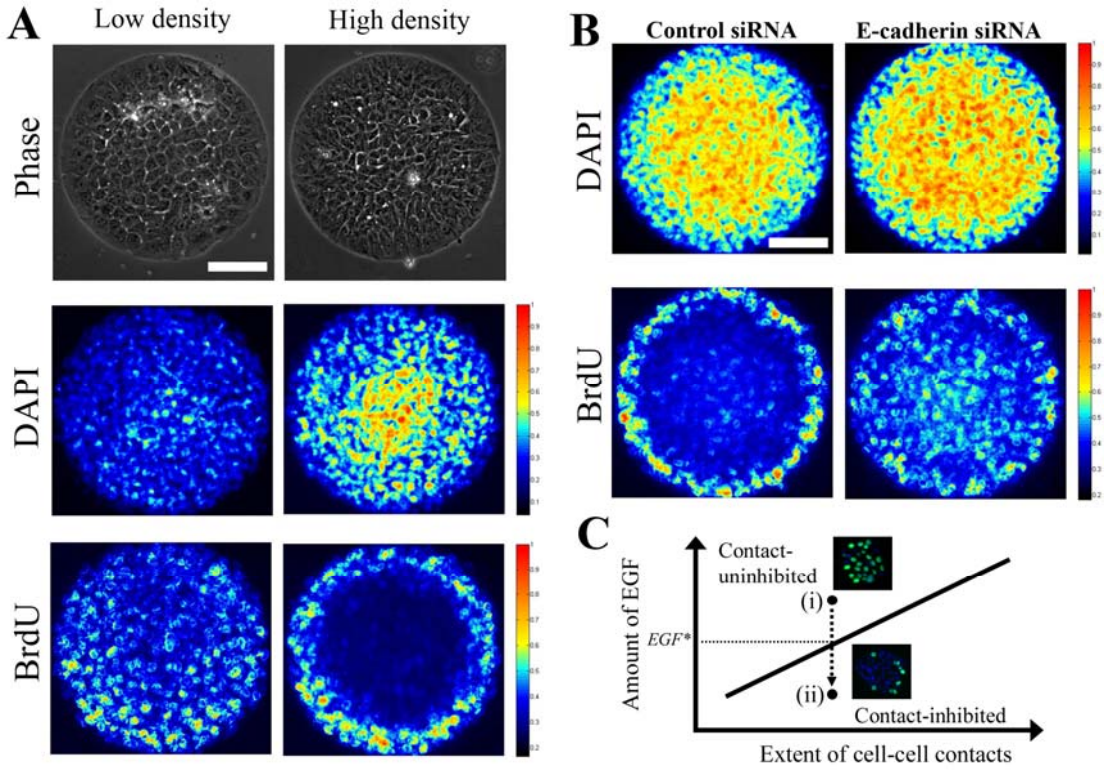

Figure 3: A quantitative balance between GFs and cell-cell contacts dictates the spatial pattern in cell cycle activity in epithelial cell clusters. (A) Low (*left*) and high (*right*) numbers of MCF-10A cells ($5x10^4$ and $1.2x10^5$ cells/cm^2, respectively) were plated on circular microdomains of the same size, serum starved for 24 h and stimulated with medium containing 20 ng/ml EGF for 24 h. By increasing the number of cells seeded, we force cells to acquire a more columnar morphology with an elevated amount of cell-cell contact area. Nuclear density (DAPI) and DNA synthesis (BrdU) was assessed by immunofluorescence. Images from 20 islands (n = 2) were stacked, and a heat map of their stacked intensities is shown. The top panel shows phase contrast images. (B) Cells treated with control or E-cadherin siRNA (50 nM) were plated at the same high density and stimulated with medium containing 20 ng/ml EGF for 24 h. Images of nuclear density (DAPI) and DNA synthesis (BrdU) were acquired from 30

islands (n = 2), and heat maps of their stacked intensities are shown. The scale bar represents 100 μm. (C) A phase diagram of epithelial cell growth as a function of growth factor and cell-cell interaction levels. Epithelial cells transition from (i) a contact-uninhibited state to (ii) a contact-inhibited state at a critical threshold level of growth factor (*EGF**). Insets show representative fluorescence images probed for BrdU uptake (green) and DAPI (blue) for clusters in contact-uninhibited and contact-inhibited phases.

To test further this phase diagram model and the tunability of the interplay between contact and GF, we revisited the relatively more straightforward scenario in which epithelial cells are growing on a non-patterned surface without any spatial constraints. According to our phase diagram model, increasing the level of cell-cell interactions in this context should enable the transition to a contact-inhibited state at higher EGF concentrations, driving the onset of the spatial pattern in cell cycle activity at an earlier time (Fig. 4A). To test this hypothesis, we retrovirally infected MCF-10A cells with either a vector encoding epitope-tagged human E-cadherin (pBabe-E-cad-HA) or an empty vector (pBabe). Cells transduced with virus encoding the exogeneous E-cadherin exhibited elevated E-cadherin expression compared to the cells infected with the virus prepared with an empty vector (Fig. 4B). Cells overexpressing E-cadherin exhibited a spatial disparity in cell cycle activity as early as 24 h at which time, non-infected MCF-10A cells (Fig. 1A, a, d) and those infected with a retrovirus encoding the empty vector exhibited a uniform growth pattern (Fig. 4C). These results reveal that the overexpression of E-cadherin induces contact-inhibition at an earlier time when EGF levels are higher, consistent with the phase diagram that we have proposed. Thus, by

tuning the level of cell-cell interactions, the spatial dynamics of epithelial proliferation may be re-engineered.

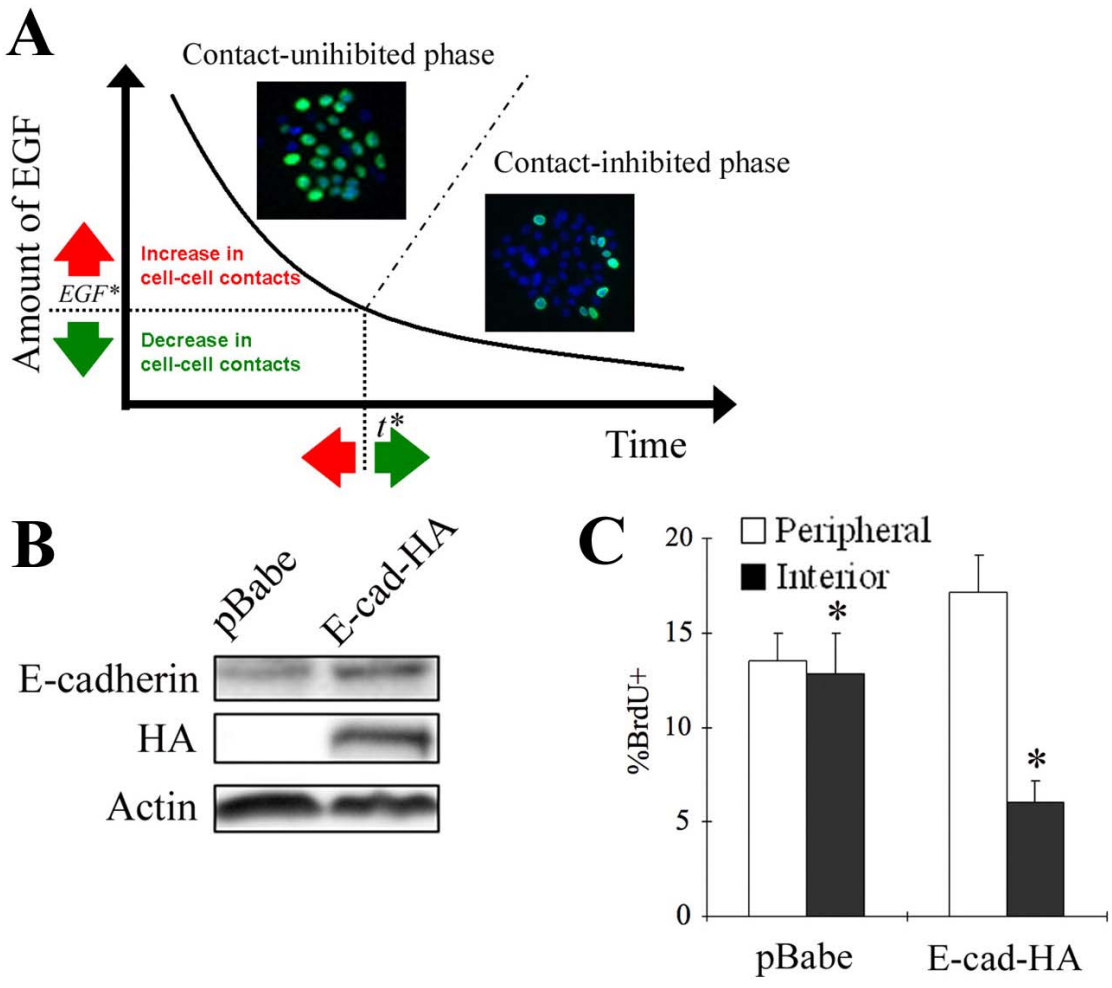

Figure 4: Spatial dynamics of epithelial growth can be modulated by tuning the critical thresholds at which contact-inhibition is triggered. (A) Model of tunable epithelial growth dynamics. Epithelial clusters grow in two modes: the first phase in which both interior and peripheral cells proliferate and a second phase in which only peripheral cells contribute to population growth. The transition from the first to second mode occurs at a threshold EGF concentration (*EGF**) at a critical time (*t**). According

to our phase diagram model, modulating the extent of cell-cell interactions should allow us to manipulate the threshold EGF concentration, and thereby affect the timing of spatial patterns in epithelial proliferation. Insets show representative fluorescence images probed for BrdU uptake (green) and DAPI (blue) for clusters in contact-uninhibited and contact-inhibited phases. (B) MCF-10A cells were retrovirally infected with the empty vector pBabe, or exogenous E-cadherin (E-cad-HA). Cells were seeded at a density of $5x10^3$ cell/cm^2, serum-starved, and treated with 0.1 ng/ml EGF. Ninety minutes later, whole cell lysates were collected, and the extent of overexpression in E-cadherin was determined by immunoblotting for E-cadherin and the epitope tag HA. Equal loading was confirmed by probing for actin. (C) MCF-10A cells infected with retrovirus encoding either the empty vector or E-cad-HA were starved and stimulated with 0.1 ng/ml EGF for 24 h. Percentage of peripheral and interior cells incorporating BrdU was quantified. Error bars indicate s.e.m. (n = 3). The *asterisk* indicates $p < 0.05$.

In summary, our quantitative measurements and analysis lead us to propose a tunable titration model for how contacts and growth factors compete to regulate cell cycle activity. This quantitative model modifies the classical notion that contact-inhibition acts as a switch that is either present or absent in normal versus tumor cells, respectively. Our findings support a more graded perspective of contact-inhibition: During cancer progression, contact inhibition may steadily erode as the threshold amount of EGF shifts lower with every genetic and epigenetic "hit." This tunability of the threshold amount of EGF would seem to be a fragility in cell cycle regulation that is exploited during cancer development. This raises the question of why this property would be preserved through

evolutionary selection. The answer may lie in its potential pivotal role in development. Theoretical models predict that an increase in cell density serves as a negative feedback that quantitatively desensitizes the mitogenic response to soluble factors, thereby self-regulating the size of developing tissues (18, 19). To our knowledge, our results provide the first experimental evidence for such a tunable, quantitative balance between contact and GFs in regulating cell cycle activity. Finally, our model indicates that epithelial clusters grow in two different modes: the first in which both interior and peripheral cells proliferate and a second mode in which only peripheral cells contribute to population growth. Manipulating cells between these modes of proliferation can provide control over population growth rate and tissue geometry, both key parameters in tissue engineering.

Materials and Methods

Cell culture and reagents

MCF-10A cells were cultured in growth medium as described previously (20). For experiments, cells were plated on either glass coverslips (VWR) or two-chambered coverslides (Lab-Tek) in growth medium for 24 h. For G_0 synchronization, cells were maintained in serum-free medium for 24 h (20). The following antibodies were used: anti-actin (Santa Cruz), anti-BrdU (Roche Applied Science), anti-E-cadherin (BD Transduction Laboratories), anti-HA (Covance), anti-phospho-Erk 1/2 (Cell Signaling Technology), anti-phospho-serine 473-Akt (Cell Signaling Technology), HECD-1 (Zymed Laboratories), mouse IgG (Sigma-Aldrich), and Alexa dye-labeled secondary antibodies (Invitrogen-Molecular Probe). The pharmacological inhibitors, PD98059 and LY294002, were obtained from Calbiochem.

Subcloning and retrovirus production and usage

The human cDNA of E-cadherin was kindly provided by P. Wheelock (University of Nebraska Medical Center), and was used to make pBabe-E-cadherin-HA construct. Briefly, the E-cadherin gene was amplified by PCR, with *Bgl*II and *Xho*I sites added to the 5' and 3' ends, respectively. In addition, to facilitate the detection of the exogenous proteins, HA epitope (YPYDVPDYA) was added to the C-terminus of the construct. The PCR product was digested with *Bgl*II and *Xho*I, and ligated into the pBabe vector. The coding sequence of pBabe-E-cadherin-HA was verified by DNA sequencing (Laragne).

Retrovirus was produced by triple transfection of HEK 293T cells and used to infect MCF-10A cells as described previously (20).

Knockdown using siRNA

siRNA targeting E-cadherin mRNAs (sense 5'-GAUUGCACCGGUCGACAAATT-3', antisense 5'-UUUGUCGACCGGUGCAAUCTT-3') was obtained from Integrated DNA Technology. Non-specific control siRNA was purchased from Ambion. siRNAs were transfected using Lipofectamine RNAiMAX (Invitrogen).

Quantification of ligand depletion

Cell number was determined by suspending cells with enzymatic treatment, and cell counting using a hemacytometer. To quantify the amount of EGF, samples from the medium were collected, pre-cleared by centrifugation and stored at -20^{o}C. EGF concentration was assayed simultaneously in all frozen samples using an enzyme-linked immunosorbent assay (ELISA) kit (R&D Systems).

Immunofluorescence and image acquisition

Fixed cells were permeabilized, blocked and sequentially incubated with primary and secondary antibodies. The cells were co-stained with DAPI (Sigma-Aldrich) or phalloidin (Molecular Probe) and mounted using ProLong Gold Antifade (Molecular Probe). Images were acquired using the Zeiss Axiovert 200M microscope. Reagents used for each type of stain are summarized in Supporting Text.

Cell lysis and Western blot

Cell lysis and Western blot were performed as described previously (20).

Fabrication of micro-patterned substrates

Fibronectin was micro-patterned on gold-coated, chambered coverslides by micro-contact printing using a PDMS stamp. Briefly, UV light was passed through a chrome mask containing the pattern (NRF at UCLA) onto a layer of SU-8 photoresist to make a mold. PDMS was cast into this mold to make the stamp. The stamp was "inked" with 16-Mercaptohexadecanoic acid (Sigma Aldrich) dissolved in 99% ethanol and was used to print gold-coated chambered coverslides. The unprinted area was passivated using PEG(6)-Thiol (Prochimia) dissolved in 99% ethanol. After washing, the coverslide was treated with EDC and Sulfo-NHS (Pierce) to activate the acid, priming it to cross-link with amine groups in fibronectin (Sigma-Aldrich).

Acknowledgements

We thank members of the Asthagiri group for helpful discussions, An-Tu Xie for his involvement in the early stages of image analysis, and Celeste Nelson and Casim Sarkar for comments on the manuscript. This work was supported by the Concern Foundation for Cancer Research and the Jacobs Institute for Molecular Engineering for Medicine.

References

1. Hanahan D & Weinberg RA (2000) The hallmarks of cancer *Cell* **100,** 57-70.
2. Steinberg MS & McNutt PM (1999) Cadherins and their connections: adhesion junctions have broader functions *Curr Opin Cell Biol* **11,** 554-560.
3. Caveda L, Martin-Padura I, Navarro P, Breviario F, Corada M, Gulino D, Lampugnani MG, & Dejana E (1996) Inhibition of cultured cell growth by vascular endothelial cadherin (cadherin-5/VE-cadherin) *J Clin Invest* **98,** 886-893.
4. Goichberg P & Geiger B (1998) Direct involvement of N-cadherin-mediated signaling in muscle differentiation *Mol Biol Cell* **9,** 3119-3131.
5. Gray DS, Liu WF, Shen CJ, Bhadriraju K, Nelson CM, & Chen CS (2008) Engineering amount of cell-cell contact demonstrates biphasic proliferative regulation through RhoA and the actin cytoskeleton *Exp Cell Res*. **314**: 2846-2854.
6. Levenberg S, Yarden A, Kam Z, & Geiger B (1999) p27 is involved in N-cadherin-mediated contact inhibition of cell growth and S-phase entry *Oncogene* **18,** 869-876.
7. Perrais M, Chen X, Perez-Moreno M, & Gumbiner BM (2007) E-cadherin homophilic ligation inhibits cell growth and epidermal growth factor receptor signaling independent of other cell interactions *Mol. Biol. Cell* E06-04-0348.
8. St Croix B, Sheehan C, Rak JW, Florenes VA, Slingerland JM, & Kerbel RS (1998) E-Cadherin-dependent growth suppression is mediated by the cyclin-dependent kinase inhibitor p27(KIP1) *J Cell Biol* **142,** 557-571.

9. Cole BK, Curto M, Chan AW, & McClatchey AI (2008) Localization to the cortical cytoskeleton is necessary for Nf2/merlin-dependent epidermal growth factor receptor silencing *Mol Cell Biol* **28,** 1274-1284.

10. Curto M, Cole BK, Lallemand D, Liu C-H, & McClatchey AI (2007) Contact-dependent inhibition of EGFR signaling by Nf2/Merlin *J Cell Biol* **177,** 893-903.

11. Lampugnani MG, Orsenigo F, Gagliani MC, Tacchetti C, & Dejana E (2006) Vascular endothelial cadherin controls VEGFR-2 internalization and signaling from intracellular compartments *J Cell Biol* **174,** 593-604.

12. Lampugnani MG, Zanetti A, Corada M, Takahashi T, Balconi G, Breviario F, Orsenigo F, Cattelino A, Kemler R, Daniel TO, *et al.* (2003) Contact inhibition of VEGF-induced proliferation requires vascular endothelial cadherin, beta-catenin, and the phosphatase DEP-1/CD148 *J Cell Biol* **161,** 793-804.

13. Weis WI & Nelson WJ (2006) Re-solving the cadherin-catenin-actin conundrum *J Biol Chem* **281,** 35593-35597.

14. Nelson CM, Jean RP, Tan JL, Liu WF, Sniadecki NJ, Spector AA, & Chen CS (2005) Emergent patterns of growth controlled by multicellular form and mechanics *Proc Natl Acad Sci USA* **102,** 11594-11599.

15. Carpenter G (2000) The EGF receptor: a nexus for trafficking and signaling *Bioessays* **22,** 697-707.

16. Liu WF, Nelson CM, Pirone DM, & Chen CS (2006) E-cadherin engagement stimulates proliferation via Rac1 *J Cell Biol* **173,** 431-441.

17. Jones SM & Kazlauskas A (2001) Growth-factor-dependent mitogenesis requires two distinct phases of signalling *Nat Cell Biol* **3,** 165-172.

18. Hufnagel L, Teleman AA, Rouault H, Cohen SM, & Shraiman BI (2007) On the mechanism of wing size determination in fly development *Proc Natl Acad Sci USA* **104,** 3835-3840.

19. Shraiman BI (2005) Mechanical feedback as a possible regulator of tissue growth *Proc Natl Acad Sci U S A* **102,** 3318-3323.

20. Graham NA & Asthagiri AR (2004) Epidermal growth factor-mediated T-cell factor/lymphoid enhancer factor transcriptional activity is essential but not sufficient for cell cycle progression in nontransformed mammary epithelial cells *J Biol Chem* **279,** 23517-23524.

Supporting Information

Quantification of immunofluorescne signals of phospho-proteins

For imaging ppErk or ppAkt, we started with a sample that is expected to give the highest FITC signal (e.g. 10 ng/ml EGF). Using this positive control, an exposure time was empirically chosen so that the highest pixel intensity in a given field is close to the saturation level (i.e. 255). The chosen exposure time was confirmed not to saturate the FITC signal in other fields of the positive control sample. These steps identify an exposure time that maximizes the dynamic range of quantification of ppErk and ppAkt. This exposure time was then used to capture images from all other samples in a given trial.

Nuclear phospho-protein signal intensity was quantified by first tracing the perimeter of each nucleus. The area and the total FITC intensity of each nucleus were determined using MATLAB. The mean background intensity per pixel was also calculated for each image from the region containing no cells. This background level was multiplied by the area of the nucleus and was subtracted from the total nuclear FITC intensity to determine the final phosphor-protein signal intensity for each nucleus.

Table 1: Details of reagents used in immunofluorescence for each stain

Application	Fixation reagents	Permeabilization	Dehydration	Blocking Solution
BrdU	70% EtOH (pH2) w/ 15 mM glycine (-20°C)	N/A	N/A	10% goat serum + 0.1% BSA in PBS
Vinculin	4% Formalin	0.2% TritonX-100	N/A	10% goat serum + 0.1% BSA in PBS
ppErk/pAkt	Freshly prepared 2% paraformaldehyde (pH 7.4) + Inhibitors[a]	0.5% NP-40 + Inhibitors	Pure MeOH (-20°C)	Blocking buffer[b]

Phosphatase inhibitors[a]: 1mM sodium orthovanadate (Sigma-Aldrich), 10mM sodium fluoride (Sigma Aldrich), and 10mM β-glycerophosphate (Sigma-Aldrich)

Blocking buffer[b]: 130 mM NaCl, 7 mM Na_2HPO_4, 3.5 mM NaH_2PO_4, 7.7 mM NaN_3, 0.1% bovine serum albumin, 0.2% Triton X-100, 0.05% Tween-20 (all from Sigma-Aldrich), and 10% goat serum (Debnath et al 2003)

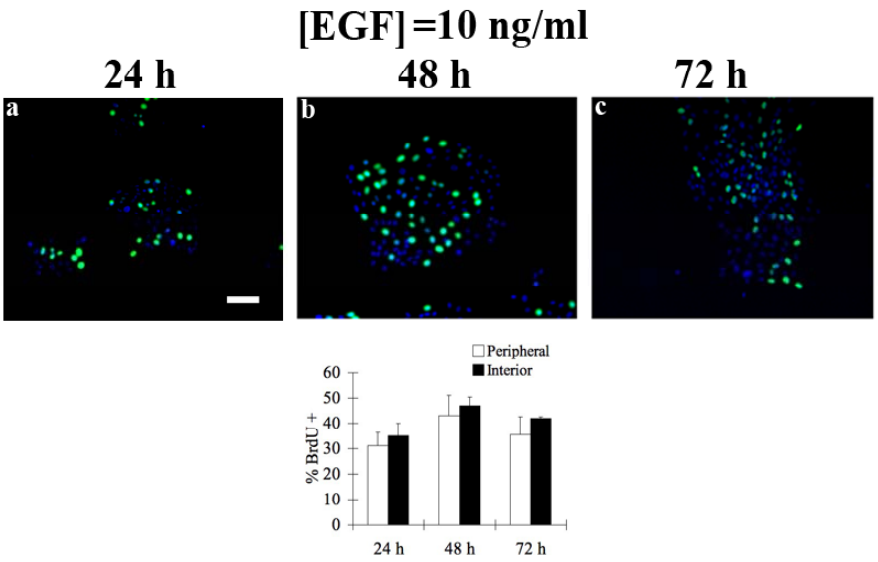

Figure S1: DNA synthesis following initial treatment with 10 ng/ml EGF. Percentage of peripheral and interior cells incorporating BrdU at 24, 48, 72 h after starved MCF-10A cells were stimulated with 10 ng/ml EGF. The *error bars* represent s.e.m. (n = 2). The scale bar represents 100 μm.

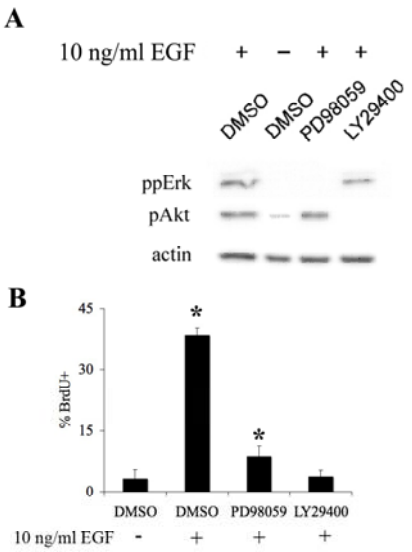

Figure S2: Erk and Akt signaling is essential for EGF-mediated proliferation of MCF-10A cells. (A) Serum-starved MCF-10A cells were pre-treated for 2 hours with PD98059 (50μM), LY29400 (50 μM), or the solvent DMSO and then stimulated with 10 ng/ml EGF or left untreated. The effect of the drugs on (A) Erk and Akt signaling pathways (15 min after stimulation) and (B) BrdU uptake (24 h after stimulation) was determined by Western blot and immunofluorescence staining, respectively. Western blotting was conducted with antibodies against ppErk (T202/Y204) and pAkt (S473), respectively. Equal loading was confirmed by probing with an anti-actin antibody. The *error bars* indicate s.e.m. (n=2). The *asterisk* indicates $p < 0.01$.

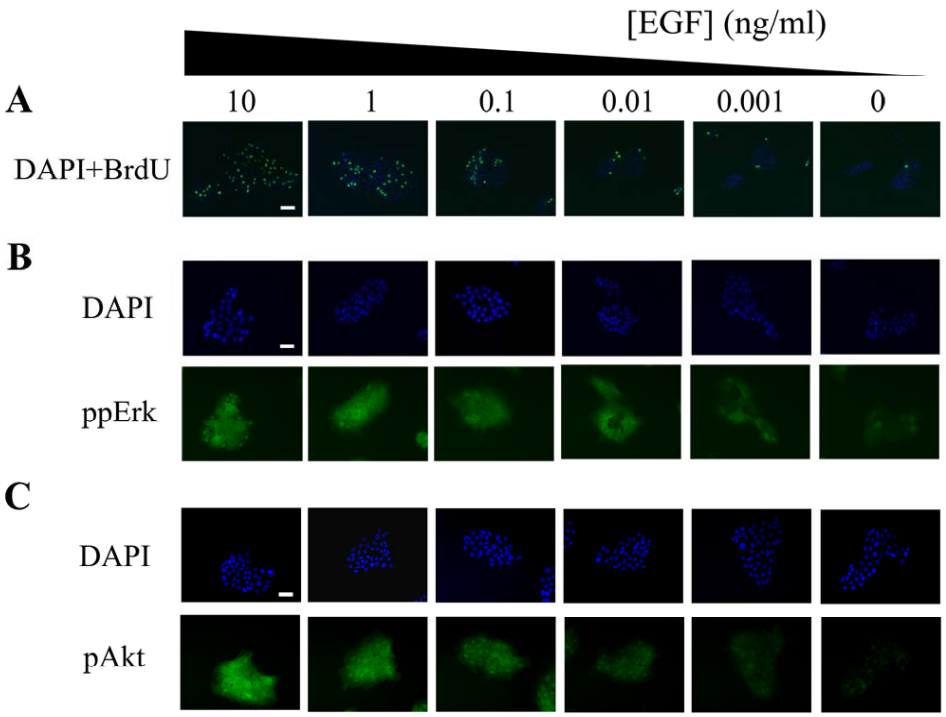

Figure S3: The effect of EGF treatment on DNA synthesis, ppErk and pAkt signals in MCF-10A cell clusters. See legend of Fig. 2 for experimental details. The scale bars represent (A) 100 and (B, C) 50 μm.

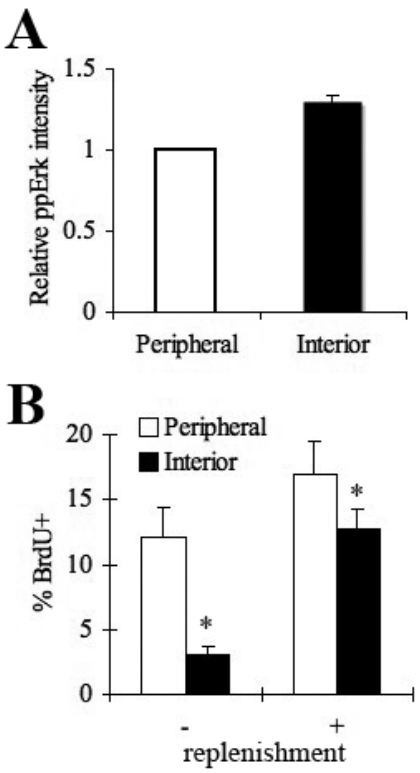

Figure S4: EGF replenishment rescues Erk signaling and cell cycle activity. (A) The level of ppErk in peripheral and interior cells following 15 min of EGF replenishment. (B) The percentage of peripheral and interior cells incorporating BrdU was quantified 24 h after medium was (+) or was not (-) replenished. The *error bars* indicate s.e.m. (n=2-5). The *asterisk* indicates $p < 0.01$.

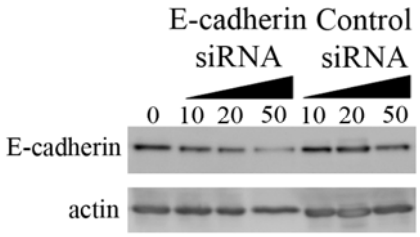

Figure S5. Effect of siRNA treatment on E-cadherin expression. Cells were transfected with control or E-cadherin siRNA in serum-free medium. The extent of knockdown in E-cadherin was determined by Western blot. Equal loading was confirmed by probing for actin.